Boronic acids for fluorescence imaging of carbohydrates

Xiaolong Sun,[a] Wenlei Zhai,[b] John S. Fossey [b] and Tony D. James[a*]

[a] *Department of Chemistry, University of Bath, Bath, BA2 7AY, United Kingdom.*

[b] *School of Chemistry, University of Birmingham, Birmingham, Edgbaston, West Midlands B15 2TT, United Kingdom.*

Contents

Abstract

"Fluorescence imaging" is a particularly exciting and rapidly developing area of research, the annual number of publications in the area has increased ten-fold over the last decade. The rapid increase of interest in fluorescence imaging will necessitate the development of an increasing number of molecular receptors and binding agents in order to meet demand in this rapidly expanding area. Carbohydrate biomarkers are a particularly important target for fluorescence imaging given their pivotal role in numerous important biological events, including the development and progression of many diseases. Therefore, the development of new fluorescent receptors and binding agents for carbohydrates are and will be in increasing demand. This review highlights the development of fluorescence imaging agents based on boronic acids being a particularly promising class of receptor given their strong and selective binding with carbohydrates in aqueous media.

Introduction

Molecular imaging, is a very important tool in life sciences and engineering, and has been a particularly fast growing area of research over the past decade. Imaging techniques have been using as powerful tools to help understanding the function and structural characteristics of tissue using intrinsic absorption and scattering *via* i*n vivo* and *in vitro* spectroscopic and microscopy techniques.[1, 2] In particular, much attention has been paid to fluorescence investigations of cells and tissues since many biochemical markers can be visualised using fluorescence contrast

agents, and they can also be targeted using appropriate fluorescent markers.[3-5] Therefore, imaging techniques are important for developing and testing novel tools, reagents, and methods to visualise specific molecular processes *in vivo*, particularly those that are key targets in disease processes.[6]

Various imaging modalities, such as positron emission tomography (PET), single photon emission computed tomography (SPECT), optical fluorescence imaging, magnetic resonance imaging (MRI), computed tomography and ultrasound imaging, and recently total internal reflection fluorescence microscopy (TIRFM), have been successfully employed in biomedical imaging.[7] Using these techniques for imaging, in conjunction with fluorescence, allows cellular events to be tracked providing biological information at the molecular level in living systems.[8] To meet the requirement for *in vivo* clinical molecular imaging, the design of highly sensitive and specific molecularly targeted imaging probes is required.[8, 9] Imaging probes are often synthesised by combining various functional moieties (i.e. radioisotopes, fluorophores, and nanoparticles) with receptors (i.e. boronic acids, macrocyclic crown ethers).[10, 11] Given the successful development of single-molecule super-resolution fluorescence imaging, precise and accurate bio-tagging and labelling can be investigated, thus potential preclinical and biomedical detection of certain diseases at an early stage may be possible in the near future.[12, 13] Fluorescence molecular imaging will allow us to answer basic *in vivo* biological questions and more importantly it could be achieved in a high-throughput fashion.[14] This review aims to capture the state-of-the-art in the emerging field of saccharide-led imaging; although still in its infancy, the authors of this report believe there is an unrealised potential for saccharide based imaging to transform the area and offer new paradigms in biomedical research.

Saccharides and Carbohydrates

Carbohydrates are vital to biological processes, and as such are important in disease diagnosis.[15] For example unregulated glucose levels in the blood and associated with diabetes, which can lead to deleterious healthcare implications such as kidney problems, heart disease, nerve damage (leading to amputations) and even blindness.[16-19] Excess blood glucose forms non-enzymatically generated conjugates and these glycated products are what led to the damage associated with diabetes. Indeed, glycated hemoglobin (HbA1c) can be monitored to give an indication of plasma glucose.[20] Such problematic glycation is more often witnessed in proteins with a long lifetimes.[21,22] Human serum albumin (HSA), the most prevalent blood protein, has a faster turnover rate than hemoglobin thus comparisons between levels of HAS and hemoglobin glycation can offer meaningful insight into time-dependant variations of blood sugar chemistry.

Glycated proteins offer the potential as disease markers and they are potential probes for diseases including certain types of cancer, Alzheimer's disease (AD), autoimmune diseases and atherosclerosis. Some of the symptoms of AD, including plaques and cell death have been linked with insulin mechanisms, because of this link in some reports the disease has been called type 3 diabetes.[23] Whilst further research remains to be carried out to back-up these hypotheses, the detection of glycated proteins has the potential to offer new diagnostic regimes for clinicians in the future. It is already known that excess Advanced Glycation End products (AGE) arising from hyperglycemia are important indicators for complications related to diabetes.[24, 25]

Table 1. Structure information on the protein[26]

Protein	**Major associated carbohydrates**

Lectin	Terminal α-1,3 mannose α-galactose, GlcNAc, α-2,3 sialic acid, β-fucose,
Ovalbumin (Oval)	Mannose, *N*-acetyl glucosamine, galactose
Bovine submaxillary mucin (BSM) Porcine stomach (PSM)	Sialic acid, *N*-acetyl glucosamine, *N*-acetyl galactose, fucose, galactose
Carcinoembryonic antigen (CEA)	Sialic acid, *N*-acetyl glucosamine, *N*-acetyl galactose, fucose, galactose, Le^X, Le^a, and Le^b antigen

Cell surface carbohydrates, as part of glycosylated proteins and lipids, have been associated with different types of cells and these surface carbohydrates present the characteristic signature of cancers' development and progression, such as sialyl Lewis X (sLe^x), sialyl Lewis A (sLe^a), Lewis X (Le^x) and Lewis Y (Le^y) (Figure 1).[27] Poly- and oligosaccharides localised on the microbial cell walls and animal cells surfaces can be targeted using sugar-specific ligands. Using these sugar-specific antibodies and lectins for controllable attachment and detachment of cells, fluorescence molecular imaging can be used for the diagnostic tracking of certain diseases or tumors.

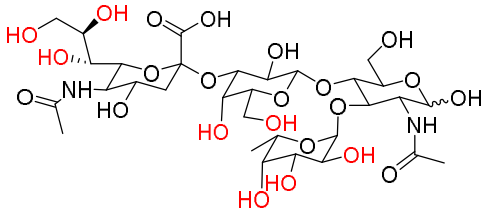

sialyl Lewis X (sLe^x)

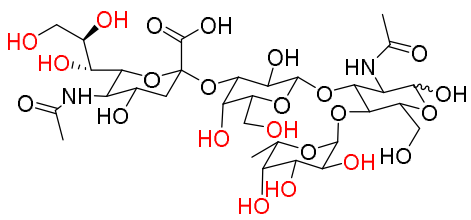

sialyl lewis A (sLe^a)

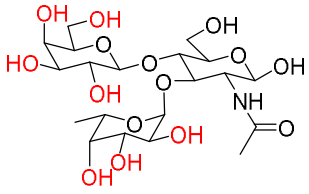

Lewis X (Le^x)

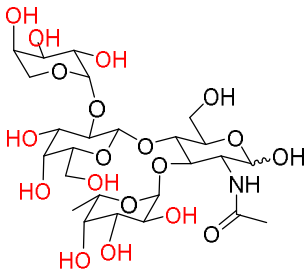

Lewis Y (Le^y)

Figure 1: *Structures of cell-surface carbohydrates, biomarkers sialyl Lewis X (sLe^x), sialyl lewis A (sLe^a), Lewis X (Le^x), Lewis Y (Le^y). The hydroxyl groups which are most likely to bind with boronic acid groups are highlighted in red. Boronic acid receptors bind reversibly to cis-1,2- and –1,3-diols, a detailed study to ascertain which diols do bind remains to be completed.*

Fluorescence for imaging applications

Since the first description of phenomenon of fluorescence by Sir George Gabriel Stokes in 1852,[28] the fluorescence-related techniques have been considered as powerful tools by chemists and biologists. Fluorescence in conjunction with microscopy can be used for the detection and visualization of biological and physiological processes and lead to a deeper understanding of diseased-specific mechanisms.[4, 10] Fluorescent probes/molecules are widely recognized as powerful sensing and imaging tools,[2, 8, 11] which have been successfully developed for a large number of biomolecules, including glutamate,[29] acetalcholine,[30] glycine,[31] aspartate[32] and dopamine.[33] Fluorescence is particularly useful to directly interrogate cell chemistry and understand the function.[34-36] The multitude of positive features, such as high sensitivity, in real-time, easy manipulation, coupled with widely available instrumentation, make

fluorescence one of the most powerful transduction mechanisms to report on chemical-biological recognition events.

Fluorescent dyes can be applied to enhance image contrast in confocal fluorescence microscopy.[37] The design of fluorescence probes with the ability to signal, sense and target carbohydrate substrates in living systems requires the optimisation of a number of factors, including chemoselectivity and bioorthogonality.[38] In the search for synthetic receptors a bottom-up design is often required, despite the apparent challenge of designing new receptors for each analyte, there are a number of recognition motifs that offer many advantages in receptor design, such as boronic acids and their ability to sequester saccharides under biologically relevant conditions.[6, 39]

Light in the Near-infrared (NIR) and Far-red region can propagate through several centimeters of tissue, therefore, in a practical sense the use of a NIR fluorescent signals to detect tumors and other diseases *in situ* and at very early stages of development is desirable.[8] It should then be possible to use imaging techniques to speed up drug screening, and to use imaging as an objective endpoint for tailoring therapies towards an individual patient.[40, 41] Therefore, the development of "smart"[42] and targeted fluorescent molecular probes with NIR emission is a particularly important area of interest.

Boronic acid for imaging carbohydrates

Boronic acids have been exploited extensively as chemo/biosensors in the detection of saccharides, anion, and reactive oxygen and nitrogen species (ROS/RNS) through electrochemical, fluorescent, and colorimetric measurements.[6, 43-47] Notably, over the physiological pH range, boronic acids are an ideal molecular receptor for 1,2- or 1,3-diols (e.g. monosaccharides) since boronic acid derivatives rapidly and reversibly interact with saccharides in aqueous media, and thus importantly the method does not consume the analyte.[48-50] Boronic acid-based molecules and boronate-modified materials have shown great utility in sensing and imaging saccharides and complex glycoproteins.[51, 52] In terms of common cell attachment and detachment protocols, boronic acid derivatives can be utilised to bind with native poly- and oligosaccharides which are present in the outer cellular wall or membrane.[53] By combining boronic acid with fluorescence dyes or Quantum Dots (QDs) or other signal reporter units, researchers have developed sensing and labeling systems for the recognition of carbohydrate biomarkers.[44] Since, the fluorescence quenching of probes is often hard to avoid, the development of effective boronic acid-based carbohydrate fluorescent sensors could be hampered. However, seminal research by Tang and co-workers has shown that aggregation-induced emission (AIE) systems based on tetraphenylethene (TPE) could be used to avoid quenching problems in the development of saccharide selective probes.[54] In this feature article, we have classified boronic acid-based fluorescent probes for carbohydrate imaging into several categories: small-molecular probes, polymer-tagged probes and benzoxaborole-based probes.

Small-molecule probes for imaging applications

Over the past decade two types of small-molecule boronate-based sensors in the imaging of carbohydrates have been used: mono-boronic acid probes and bisboronic acid probes. Noticeably, bisboronic acids are more widely used due to the increased number of binding sites for interaction with carbohydrate bio-markers.[6, 55] The increased number of binding sites between the boronic acid receptor and carbohydrates results in a strong binding affinity and hence improved labeling or imaging of the target carbohydrate.[49, 50, 56] For example, in 2002, Wang and co-workers[57] designed and synthesised a series of fluorescent bisboronic acid probes by changing the linker between the bisboronic acid units, producing receptors for the detection of sialyl Lewis X (sLe^x). Among them, compound **1** with the strongest affinity for sLe^x displayed specific labeling of sLe^x-expressing HEPG2 cells, whilst non-sLe^x-expressing cells were not labeled in the control experiment (Figure 2).

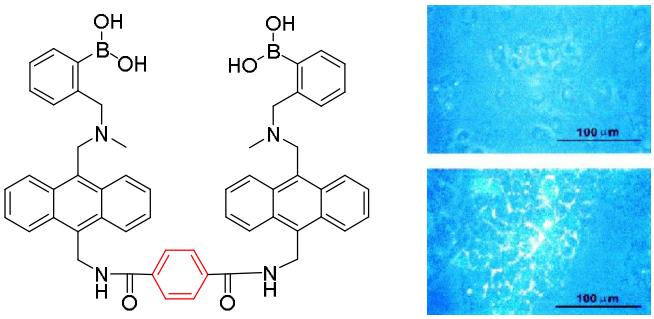

1

Figure 2. *Structure of compound **1** and fluorescent labeling studies of sLe^x-expressing HEPG2 cells (bottom) and non-expressing COS7 cells (top) with compound **1** (5 µM). Reproduced with permission from (Bioorg. Med. Chem. Lett., 2002, 12, 2175). Copyright © 2002 Elsevier Ltd.*

Wang and co-workers[58] have also evaluated compound **1** and compound **2** for the selective labeling of cell-surface sLe^x (HEPG2 cells) over Lewis Y (HEP3B cells). With detection levels for sLe^x of 0.5 to 10 µM using compound **1** (5 µM), and resulting in the specific imaging of HEPG2-expressed sLe^x over HEP3B-expressed Lewis Y (Figure 3). However, the specific binding mode between probe **1** and sLe^x which produces this selectivity was not well understood.

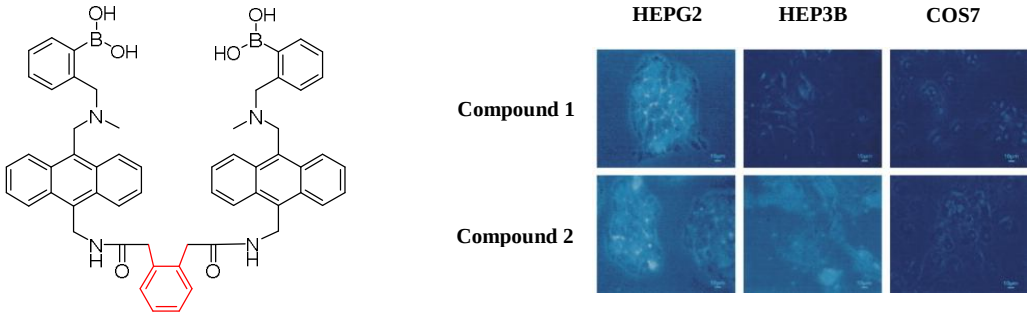

2

Figure 3. *Structure of compound **2** and fluorescent Labeling Studies of HEPG2, HEP3B, and COS7 Cells by using compound **1** and **2**. HEPG2 cells express only sLe^x, HEP3B cells express only Lewis Y, and COS7 cells do not express either antigen. Reproduced with permission from (Chem. Biol., 2004, 11, 439). Copyright © 2004 Elsevier Ltd.*

Based on Wang's work, a similar bisboronic acid receptor was developed by Craig.[59] Three bisanthracene bisboronic acid derivatives were investigated (compounds **1**, **3** and **4**), with binding affinities towards D-fructose of 212 M^{-1}, 266M^{-1} and 504 M^{-1} respectively and binding constants towards D-glucose of 28 M^{-1}, 1 M^{-1} and 2 M^{-1} respectively. The compounds were used for labeling liver carcinoma cells HEPG2 and a normal fibroblast mammalian cells COS-7, the non-labeled cells presented as grey images and labeled cells can be seen with a blue color in their images. The staining results shown in Figure 4 indicate that both compound **1** and **3** stain the HEPG2 cells and compound **1** stained COS-7 cells while compound **4** showed weak or no binding affinity for either cell line. The non-selective labeling when using compound **1** is in contrast to the earlier work which indicated specificity toward hepato-cellular carcinoma cells *versus* normal fibroblast cells.

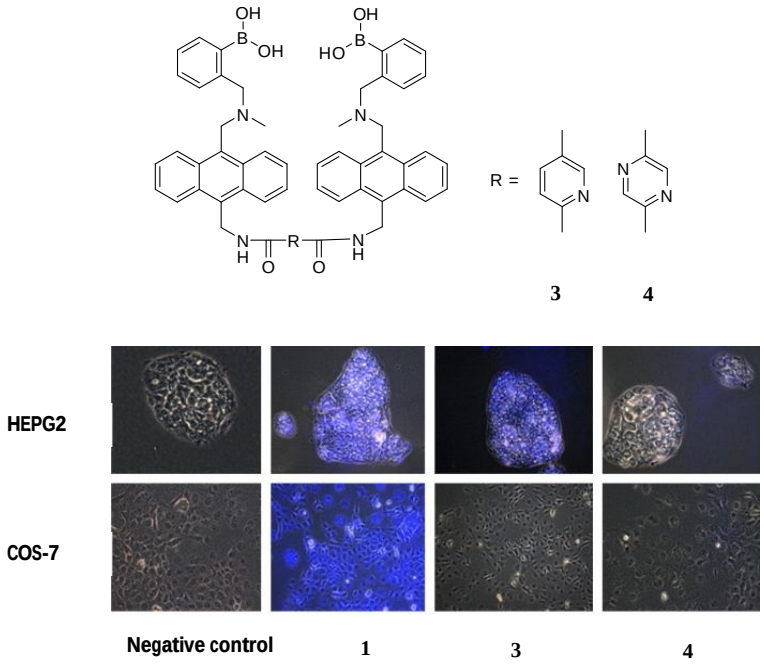

Figure 4. *Structures of compound **3** and **4**. Fluorescent labeling studies of a liver carcinoma cell line HEPG2 and a normal fibroblast mammalian cell line COS-7 with compounds **1**, **3** and **4**. The negative control contains buffer only. Reproduced with permission from (Bioorg. Chem., 2012, 40, 137). Copyright © 2012 Elsevier Ltd.*

In extending this work, Wang and co-workers[60] have linked the carbohydrate biomarker-targeting small molecule **1** and matrix-free MALDI mass spectrometric tag using click chemistry to produce the boronolectin-trityl reporter **5**. The new system was used to track cancer cell surface sLe^x expression in freshly-frozen renal tissues. Figure 5a shows that the system can specifically bind only in the region of the tumor with sLe^x expression, and also in alcohol fixed renal tumor tissue (Figure 5b). The mass spectrometric probe was exploited in the MALDI-based imaging of cancer based on its cell surface carbohydrate.

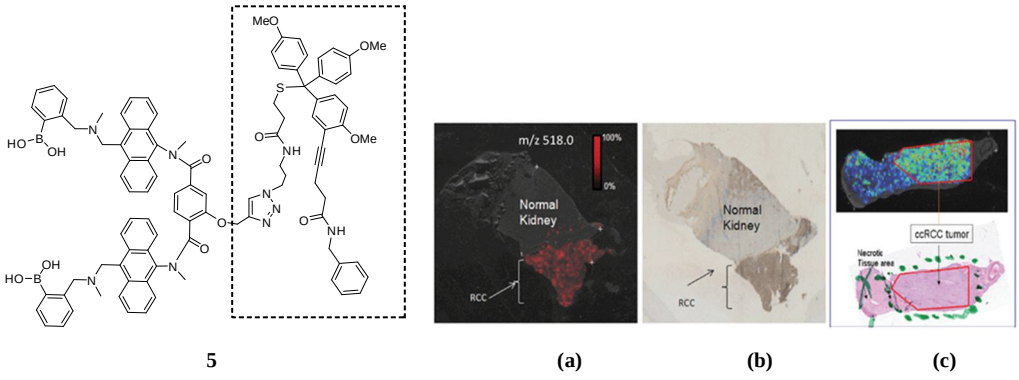

Figure 5. *(Left) Structure of compound **5**. (Right) (a) MALDI-IMS and (b) immunostaining images of kidney tissue. Immunostaining and MALDI-IMS-boronolectin signal results overlap in the tumor region, not in the normal cell areas. (c) Boronolectin staining of a Sakura/UMFix alcohol fixed renal tumor tissue. Reproduced with permission from (Chem. Commun., 2011, 47, 10338). Copyright © 2012 Royal Society of Chemistry.*

In the recent work, Wang has reported that the over-expressed carbohydrate-based carcinoma biomarker, sialyl Lewis X was selectively labeled in the mouse xenograft tumor *via* a novel boronolectin-fluorophore **6**.[61] The fluorescent agent (Figure 6A) was injected *via* the tail vein into a mouse with xenograft (sc) tumor for fluorescent imaging. As can be seen from Figure 6B, after 24h washing period, compound **6** could be used to target a tumor.

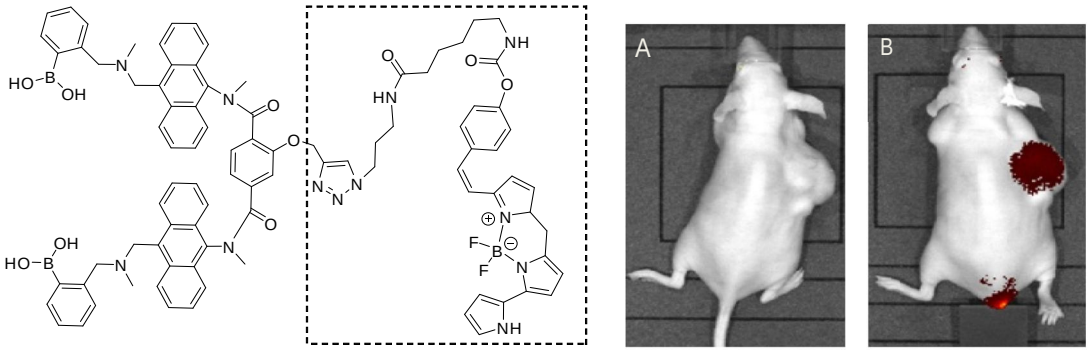

6

Figure 6. *Structure of compound **6** and its optical imaging of xenograft tumors by specific boronolectin-fluorophore **6**, (A) mouse before imaging agent injection; (B): mouse 24 h after tail vein injection of the contrast agent showing almost exclusive delivery to the tumors site. Reproduced with permission from (Bioorg. Med. Chem. Lett. 2013, 23, 6307). Copyright © 2013 Elsevier Ltd.*

Above all, in Wang's systems, compound **1** showed the most promising results for the binding with the important cancer-cell related biomarker sLe^x. The system has been further improved with the development of **5**, **6** derived from compound **1**, which have been successfully used for the imaging and labeling of carbohydrate-based biomarkers in cells and tissues.

In the design of bisboronic acid system, peptides are versatile molecules with high biocompatibility and excellent water-solubility and can be used to target cancer cell detection and cancer diagnosis. Including binding with over-expressed bioactive sequences such as arginine-glycine-aspartic acid and its receptors (integrins of $\alpha_v\beta_3$ and $\alpha_v\beta_5$). For these reasons, peptide-based linkers have been widely employed in the construction of cancer specific receptor units. Therefore, functionalisation with boronic acid derivatives at different positions along the peptide back bone, has resulted in new sensing and labeling probes for the *in situ* recognition of cell-surface glycans for the targeted imaging of cancer cells.

Lavigne and co-workers[26] have prepared bisboronic acid-appended peptide library using a biased split-and-pool combinatorial approach (Figure 7), the so-called peptide boronolectins (PBL) have been bound to beads and used for binding cancer related targets, such as oligosaccharide and glycoprotein. To investigate the ability of the peptides library to bind glycans, fluorescently labeled glycoproteins (FITC) including ovalbumin (Oval), bovine submaxillary mucin (BSM), and porcine stomach mucin (PSM) were assayed through color analysis output for each bead on an 8-bit scale and as revealed by the microscope images from Figure 8, the differential binding between different glycoproteins with peptide was observed which indicated the strong affinity between the bisboronic acid peptide receptors and the glycoproteins.

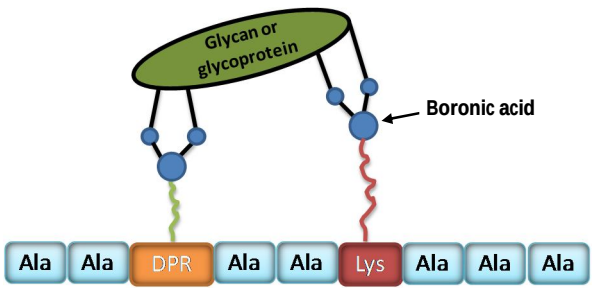

Figure 7. *Schematic representation of a phenylboronic acid substituted peptide (PBL, sequence chosen at random from ten amino acids) binding to a glycan or glycoprotein.*

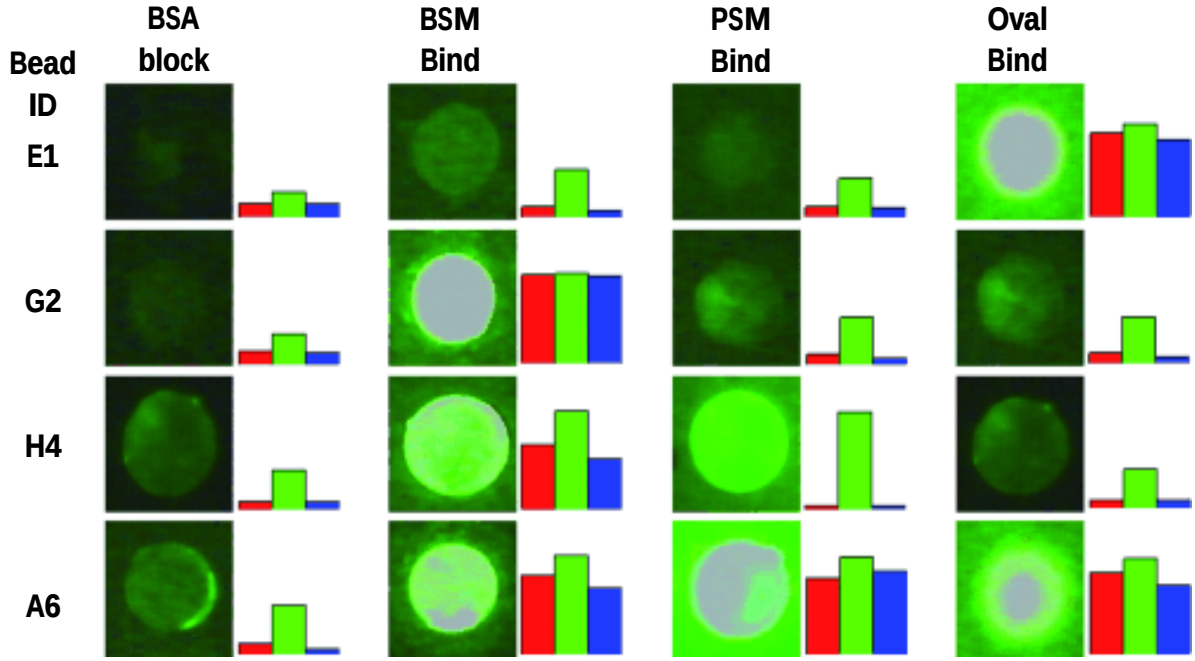

Figure 8. *Microscope images of individual beads responding to FITC-labeled glycoproteins (BSA 1% w/v; Oval, 100 μg mL^{-1}; BSM, 500 μg mL^{-1}; PSM, 500 μg mL^{-1}) and the subsequent color (RGB) output analysis to the right of each image. The beads chosen represent selective (E1, G2), partially cross-reactive (H4), and completely cross-reactive (A6) library members. Reproduced with permission from (Chembiochem, 2007, 8, 2048-2051). Copyright © 2007 WILEY-VCH Verlag.*

Bisboronic acid-functionalised peptide-based fluorescent sensors (BPFSs) have been prepared by Zhang and co-workers.[62] They synthesised five BPFSs by incorporating anthracene-phenylboronic acid within different peptide chains (Figure 9). Those kind of sensors were then applied *in situ* recognition of cell-surface sLe^x and integrins for fluorescent imaging of target cells (Figure 9). In Figure 9 (B-E), fluorescence intensity of the cells increased as the incubation time between hepG2 cells and BPFS$_1$ increasing by observing confocal laser scanning microscopy (CLSM) images. However, both the input of antibody and using BPFS1 analogue without boronic acid group into the cells keep the fluorescence intensity very low (Figure 9F$_1$, 9G$_1$). These structure-based screening processes demonstrated the specific recognition of cell-surface sLe^x using phenylboronic acid groups and those sensors were promising for the selective labeling of cell-surface glycans of human hepatic cancer cells.

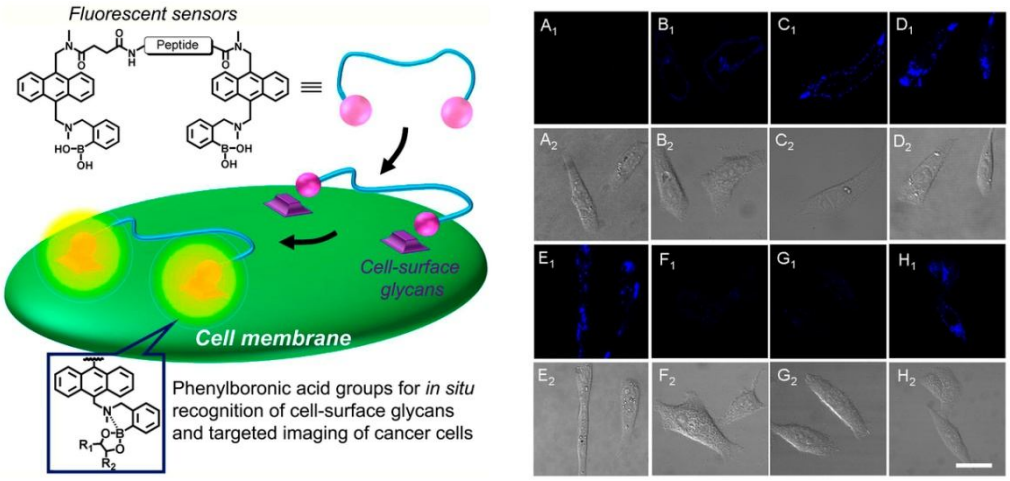

Figure 9. *(Left) Schematic presentation of BPFSs for in situ cancer cell recognition and imaging. (Right) (A): CLSM images[63] of HepG2 cells incubated in free culture medium; (B–E): CLSM images of HepG2 cells incubated with BPFS1 (20 μM) for 1 min (B), 3 min (C), 5 min (D) and 10 min (E); (F): CLSM images of HepG2 cells incubated with the antibody of CSLEX-1 for 15 min and then further incubated with BPFS1 (20 μM) for another 5 min; (G): CLSM images of HepG2 cells incubated with BPFS1 analogue (20 μM) without phenylboronic acid groups for 10 min; (H): CLSM images of HepG2 cells incubated with BPFS4 (20 μM) with a peptide sequence of FAGDF for 5 min. A1–H1: confocal fluorescence field images; A2–H2: bright field images. Reproduced with permission from (Sci. Rep. 2013, 3, 2679). Copyright © 2013 Nature Publishing Group..*

Schepartz and co-workers[64] evaluated a rhodamine-derived bisboronic acid RhoBo **7** (initially prepared as a monosaccharide sensor[65]) binding with peptides with 2-4 serine residues (each serine group presents a hydroxyl group for binding with the boronic acid receptor). Through testing different peptide sequences, it is observed that the RhoBo **7** formed the highest affinity complex with peptide containing the sequence Ser-Ser-Pro-Gly-Ser-Ser in buffer at 37 °C. Furthermore, they used Rhobo **7** to image tetraserine-containing proteins on saccharide-rich cell surface in the cytosol using epifluorescence (Epi) and total internal reflection fluorescence microscopy (TIRFM) clearly demonstrating that tetraserine could be selectively complexed and imaged even in the presence of saccharides. Figure 10 shows that only cells treated with RhoBo **7** show a significant signal (emission at 520 nm, no fluorescence signal without RhoBo) inside the cell with maximum intensity in the nucleus and outer plasma membrane (Figure 10B). These phenomena suggested that RhoBo is a selective small-molecule tag for tetraserine-containing protein on and within living cells through high affinity complex formed with bisboronic acids.

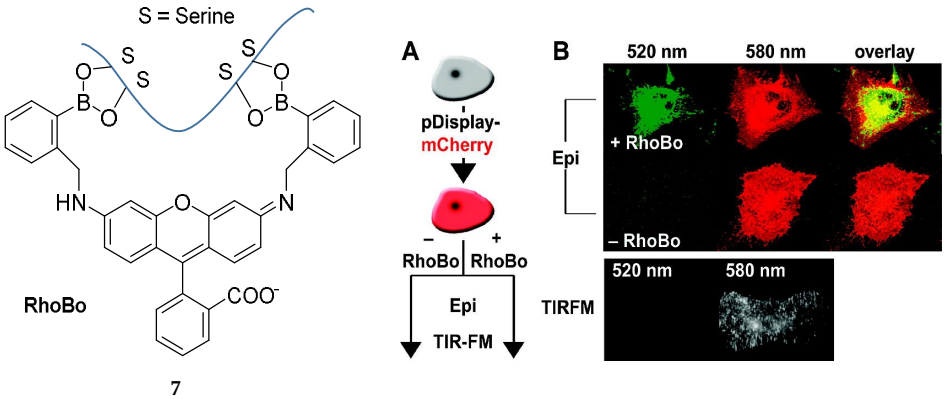

Figure 10. *(A) Experimental strategy to evaluate the extent of cell surface labelling by RhoBo. HeLa cells were transfected with pDisplay-mCherry (emission maximum 580 nm), incubated in the presence or absence of RhoBo (1 μM) (emission maximum 520 nm), and (B) imaged using epifluorescent and TIRF microscopy. Reproduced with permission from (J. Am. Chem. Soc. 2009, 131, 438). Copyright © 2009 American Chemical Society.*

Given the advantages of bisboronic acid-tagged peptides for the targeting and sensing of cell-surface biomarkers, it

may be reasonable to assume the area will be further developed resulting in the design and development of systems for bio-imaging applications. Moreover, multiple boronic acids-tagged peptides would be further developed and applied in the sensing, targeting and labeling polysaccharides, or disease-related biomarkers.

The next different example is using mono-boronic acid-based small-molecular fluorescent probe, Gois[66] has developed fluorescent 2-acetylbenzeneboronic acids **8** and **9** that undergo B–N promoted conjugation with lysozyme and *N*-(2-aminoethyl) folic acid (EDA-FA), resulting in conjugates that are selectively recognised and endocytosed by NCI-H460 cancer cells only when it over-expressed folic acid receptors (Figure 11). While in the control experiment lacking the boronic acid functionality hardly formed the expected constructs with the protein which highlight the contribution of boronic acid to imine stabilisation and internalisation of the conjugation.

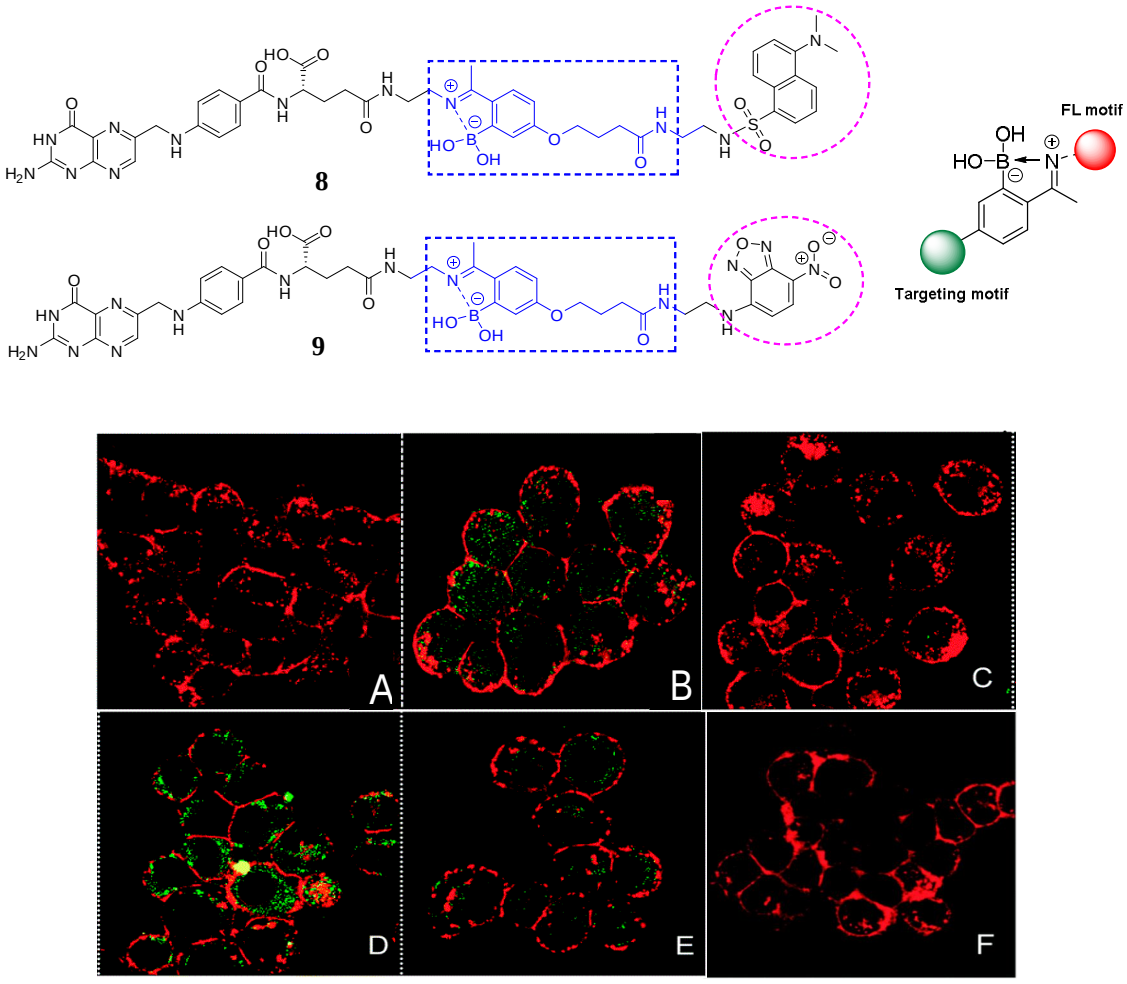

Figure 11. *Proposed structure of N–B based cancer cell targeting fluorescent conjugates **8** and **9**. Optical imaging of xenograft tumor by specific boronolectin-fluorophore. (A): HEK and (B): NCI-H460 cells were incubated with compound **8**; (C) NCI-H460 and (D) NCI-H460 without and (E) with pre-treatment with EDA-FA were incubated with compounds **9**; (F) NCI-H460 treated with no boron compound. Images show an overlay of the emission of compounds in the 460–580 nm regions upon excitation at 458 nm (green), and the emission of the membrane marker in the 650–700 nm regions upon excitation at 514 nm (red). Reproduced with permission from (Chem. Commun., 2014, 50, 5261). Copyright © 2014 Royal Society of Chemistry.*

Zhang and co-workers developed a peptide nanofibrous indicator (NFI) for naked eye-identification of cancer cells.[67] The nanofibrous indicator was prepared by mixing a borono-peptide (BP) with Alizarin Red S (compound 10). The nanofibrous self-assembly of BP/ARS produced *β*-sheets which can be dissociated by the addition of targets with higher binding affinities for the boronic acid than ARS (ie. monosaccharides and cell-surface carbohydrates overexpressed on certain cancer cells). The indicator displacement assay (IDA) system was evaluated both *in vivo* and *in vitro* allowing the naked-eye evaluation of cancer cells, using boronic acid binding with HepG2 cell-surface sLex (Figure 12). As can be seen from Figure 12A and 12C, the specific recognition between the boronic acid NFI

and cell-surface sLex resulted in a weak fluorescence from ARS released from the BR/ARS complex. While HepG2 and COS7 cells showed a strong red fluorescence (Figure 12B and 12D), indicating that the BP and ARS can be internalized and combine with each other to form a fluorescent BP/ARS complex.

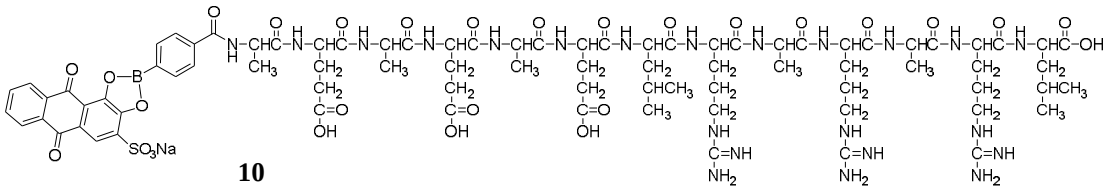

10

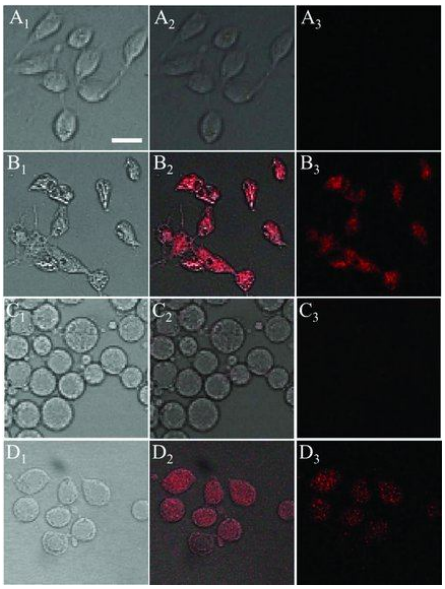

Figure 12. *Confocal laser scanning images of HepG2/COS7 cells co-incubated with the NFI and with BP followed by the addition of ARS. A $_{1–3}$) HepG2 cells co-incubated with the NFI; B $_{1–3}$) HepG2 cells co-incubated with BP and then ARS added; C $_{1–3}$) COS7 cells co-incubated with the NFI; D $_{1–3}$) COS7 cells co-incubated with BP and then ARS added. Reproduced with permission from (Small **2013**, 9, 920). Copyright © 2013 WILEY-VCH Verlag.*

Polymer-tagged boronic acid probes for imaging application

A significant enhancement in the binding of saccharide containing biomolecules, and hence the performance of a sensor system, can be achieved by incorporation of boronic acid units into a polymer matrix.[6, 68, 69] Boronic acid-containing polymers have been found out valuable in a variety of biomedical applications, including treatment of HIV,[70, 71] obesity,[72, 73] diabetes,[6] and cancer.[74, 75] Inclusion of the molecular sensor in the polymer can help in the development of superior analytical devices for carbohydrate imaging, since the polymer imparts many advantages such as improved robustness, sensitivity, handling, and biocompatibility. These properties are vital for the development of noninvasive biomolecular imaging tools. [76, 77]

In the design of a novel stimuli-responsive controlled-release system, Lin and co-workers[78] visualised intracellular delivery of both insulin and cAMP (cyclic adenosine monophosphate) by using a 8-Fluo-cAMP-loaded BA-MSN particles (boronic acid-mesoporous silica nanoparticle) that can internalise within live RIN-5F cells (Scheme 1). The importance of this work is to overcome the difficulty of control of intracellular cAMP delivery by a drug carrier. By the introduction of saccharides (Figure 13b-c), green fluorescence in fluorescence confocal micrographs was clearly observed for both Fluo-cAMP-loaded BA-MSN particles and the free Fluo-cAMP molecules released from the MSN intracellularly by interaction of the boronic acid with glucose in live mammalian cells (Figure 13).

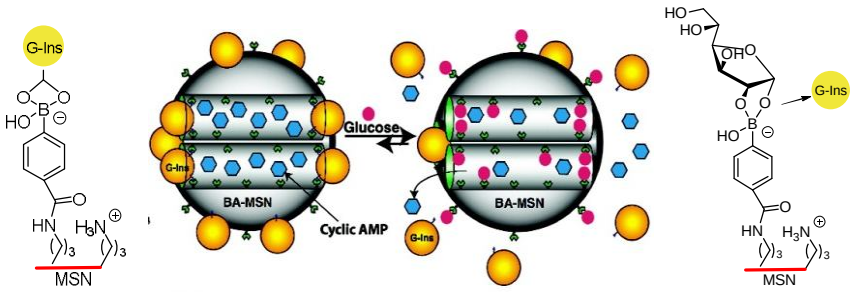

Scheme 1. *Schematic representation of the glucose-responsive MSN-based delivery system for controlled release of bioactive gluconic acid-modified insulin (G-Ins) and cAMP.*

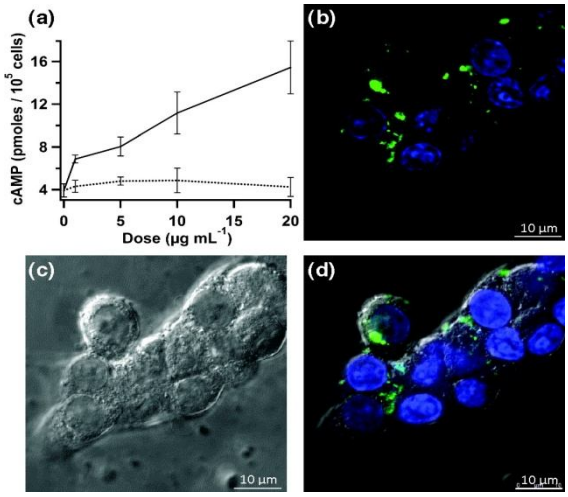

Figure 13. *(a) Intracellular cAMP concentration of rat pancreatic RIN-5F cells treated with the cAMP-loaded BA-MSN (solid line) and free-solution cAMP (dashed line), measured after 6 h of introduction; (b) Fluorescence confocal micrograph of RIN-5F cells incubated with 20 μg mL^{-1} Fluo-cAMP-loaded BA-MSN (green) for 6 h.. Cell nuclei were stained with DAPI (blue). (c) Corresponding differential interference contrast (DIC) micrographs. (d) Fluorescence confocal and DIC merged image. Reproduced with permission from (J. Am. Chem. Soc. 2009, 131, 8398). Copyright © 2009 American Chemical Society.*

To make fluorescent glucose probes developed from QDs more practical for intracellular imaging, modified CdTe/ZnTe/ZnS core/shell/shell (CSS) QDs bearing phenylboronic acid (PBA) were prepared by Zhou *et al*. through attaching PBA-functionalised groups to QDs surface (Figure 14a).[79] To monitor the glucose-mediated assembly of PBA-QDs, dynamic light scattering (DSL), TEM images were used to characterize the changes of QDs properties before and after the addition of glucose. The unique glucose-mediated assembly of PBA-QDs could be used to modulate the photoluminescence (PL) properties of the QDs and results in a selective ratiometric response towards glucose (Figure 14a). The ability of the PBA-QDs to enter cells and detect intracellular glucose levels in mouse melanoma B16F10 cells (grown in sugar-free Dulbecco modified Eagle medium) was then tested. When B16F10 cells were treated with PBA-QDs, a cross-sectional Z scan confirmed the entry of the QDs into the cells (Figure 14b left). A continuous irradiation assay confirmed the photostability of the QDs in the cells. Subsequently the cells were fed with different amounts of glucose, and the emission maximum of PBA-QDs shifted from 590.2 nm to 596.7 nm and 609.8 nm corresponding to glucose at concentrations of about 4.0 and 15.9 mM, respectively (Figure 14b). Thus, the unique glucose-mediated assembly of PBA-modified QDs could be applied for a selective ratiometric response to glucose through modulating the PL properties of QDs in living cells.

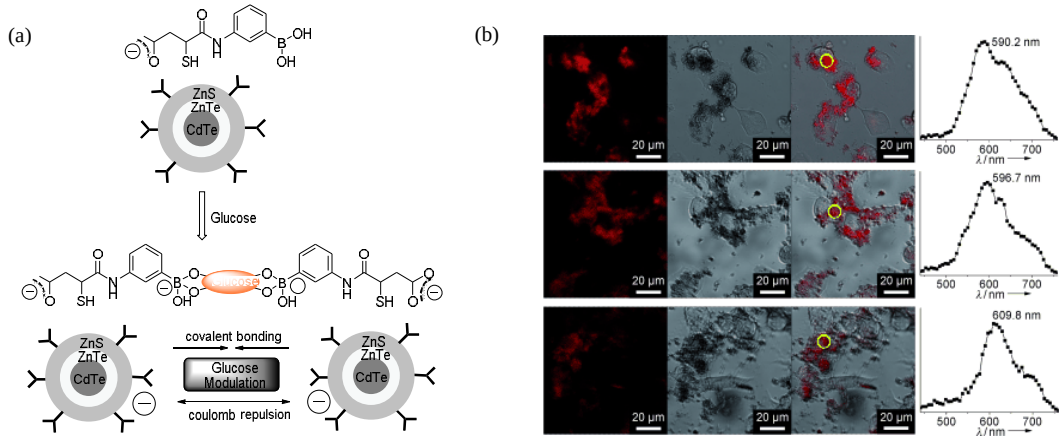

Figure 14. (a) *Glucose-mediated assembly of PBA-modified CdTe/ZnTe/ZnS CSS QDs; (b) Scanning confocal fluorescence microscopy images (left), transmission microscopy images (center), and overlaid images (right) of mouse melanoma cells B16F10 incubated with PBA-QDs (5.0 mg mL^{-1}), with the additional feeding of glucose at concentrations. The local PL spectra were obtained from the regions within the yellow circles. Reproduced with permission from (Angew. Chem. Int. Ed. Engl.,* ***2010****, 122, 6704). Copyright © 2010 WILEY-VCH Verlag.*

It is always challenging to design a fluorescence-based system for continuous glucose monitoring (CGM) *in vivo* even though it is so important to break through the difficulties. To overcome the barriers, an injectable hydrogel fashioned into microbeads, which incorporates an established glucose selective fluorescent sensor (GF-hydrogel) was reported for the first time by Takeuchi and co-workers (Figure 15 Left). The glucose-responsive bead (GF) system demonstrated highly-sensitive, bio-stable, long-lasting, and injectable properties for *in vivo* continuous glucose detection (Figure 15 Right). Significantly, the fluorescence intensity of the injected GF-beads was transdermally detectable and visible through the ear skin of mice without any abnormalities for over 30 days (Figure 15A-B). They also experimentally verified the correlation between the fluorescence intensity of the implanted GF-beads and the *in vivo* blood glucose concentrations (370 mg·dL^{-1} – 130 mg·dL^{-1}, modulated by insulin) by nine intravenous glucose infusions and found out that fluorescence intensity of the microbeads could be used to accurately monitor the blood glucose concentrations (Figure 15C-G).

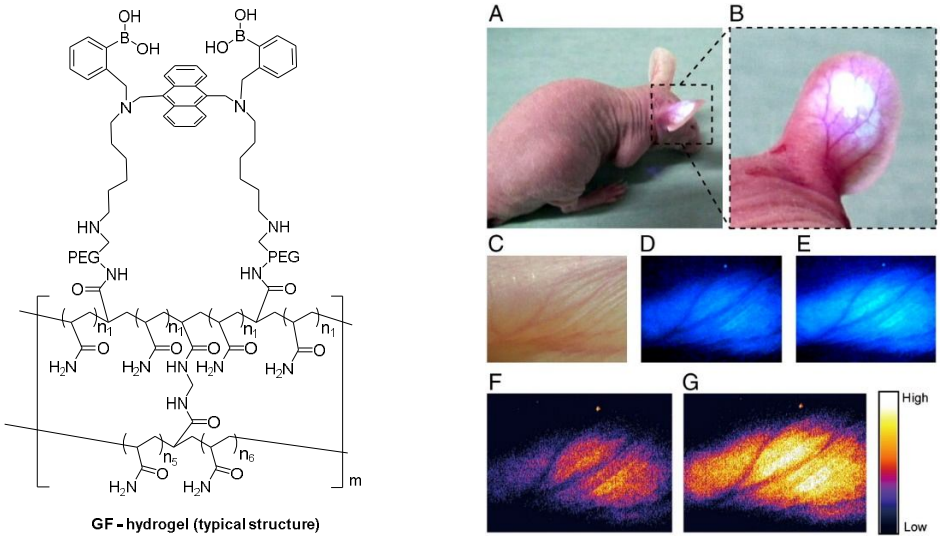

Figure 15. *(Left) Typical structure of GF-polyacrylamide hydrogels; (Right) In vivo CGM in a mouse using injected GF-beads. (A, B) glucose responsive fluorescence beads under the dermis of a mouse ear. (C) Enlarged view of the implantation site in the mouse ear. (D, E) Fluorescent images for glucose concentration within the euglycemic and hyperglycemic ranges, respectively. (F, G) Pseudocolored images of D and E. Reproduced with permission from (Proc. Natl. Acad. Sci. U.S.A* ***2010****, 107, 17894) Copyright © by the National Academy of Sciences.*

In order to address two limitations: i) that continuous glucose monitoring may not be required over the

whole lifetime of the subject and ii) that the microbeads slowly disperse, they have moved to a more robust and easily removable fiber sensor system.[80] The fiber material consists of polyethylene glycol (PEG)-bonded polyacrylamine (PAM) hydrogel and incorporates the same sensor unit.[81] In their smart structure design, polyethylene glycol (PEG)-bonded polyacrylamide (PAM) hydrogel fibers (better performance than PAM hydrogel fibers) were employed since they can reduce inflammation and continuously respond to blood glucose changes for up to 140 days. The fiber system can be used for long-term *in vivo* glucose monitoring, fibers still showed a very strong fluorescence signal through ear skin even one month after implantation (Figure 16). These fibers can also be implanted and removed quickly and simply (Figure 17), which has the additional advantage that maybe unknown long-term side effects are not given the chance to manifest.

Figure 16. *Inflammation induced by the implanted fibers and transdermal transmission over a long period. The comparison of fluorescence intensity of the PAM hydrogel fibers with and without PEG through the ear skin for one month. Reproduced with permission from (Proc. Natl. Acad. Sci. U.S.A 2011, 108, 13399) Copyright © by the National Academy of Sciences.*

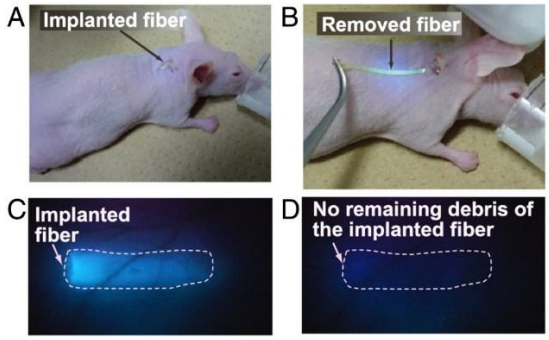

Figure 17. *The implanted fiber can be easily removed from the implantation site after use. (A) Fiber implanted into the mouse ear. (B) The implanted fiber was easily removed from the ear. (C) Fluorescence image of the mouse ear before removing. (D) Fluorescent image after fiber removal. Reproduced with permission from (Proc. Natl. Acad. Sci. U.S.A 2011, 108, 13399) Copyright © by the National Academy of Sciences.*

In addition, Elsen has demonstrated that glycated proteins can be visualized and identified in a variety of complex biological samples, including human serum, Manduca sexta hemolymph and mouse brain cortex homogenates, using fluorescent boronic acids in Flu-PAGE and Flu-BLOT.

Benzoxaborole-based probes for saccharide imaging applications

Dennis Hall pioneered the use of the benzoxaborole **11** (*ortho*-hydroxymethyl phenylboronic acid) receptor which has been shown to be a superior receptor unit to the well-established dialkylamino boronic acids (Wulff type, compounds **1** - **9**) analogues.[83] The benzoxaborole **11** unit binds strongly with 4,6-diols and as such can be used to complex strongly with cell-surface glycoconjugates.[84]

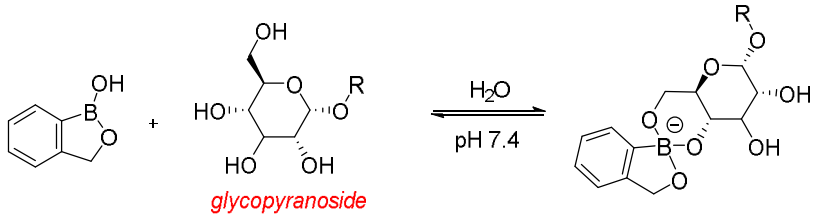

11

Scheme 2. *Reversible covalent bonding between benzoborole and glycopyranoside.*

Inefficient cellular delivery limits the application of macromolecular drugs.[85, 86] Therefore, through the targeting of therapeutic agents to the glycocalyx, it is anticipated that this would enhance the cellular delivery of the drug. In order to evaluate this concept, Raines has conjugated benzoxaborole moieties with bovine pancreatic ribonuclease (RNase A) and used the enhanced affinity towards: D-fructose, D-glucose and *N*-acetylneuraminic (Neu5Ac) to aid intracellular targeting of the conjugate.[87] In the design, 5-amino-2-hydroxymethylphenylboronic acid was linked *via* an amide bond to the protein carboxyl groups using a carbodiimide coupling agent (Figure 18a). A fluorophore-labeled protein and flow cytometry was used to quantify cellular internalisation. Chinese hamster ovary cells (Lec-2) were employed since they have lower levels of sialic acid in their glycocalyx than their progenitor line (Pro-5). This experiment was designed to determine whether the conjugated benzoxaborole would elicit selectivity for cells with higher quantities of cell-surface sialic acid since sialic acid is of high abundance in the glycocalyx. It is found out that boronation of RNase A increased its cellular uptake by 4 to 5-fold (Figure 18b). Thus, it was shown that the boronated protein has enhanced affinity for *in vitro* oligosaccharides and also facilitates cellular uptake of the protein and enhances protein delivery to the cytosol. It was concluded that such benzoxaborole have many attractive attributes and could be used as ideal mediators in drug delivery.

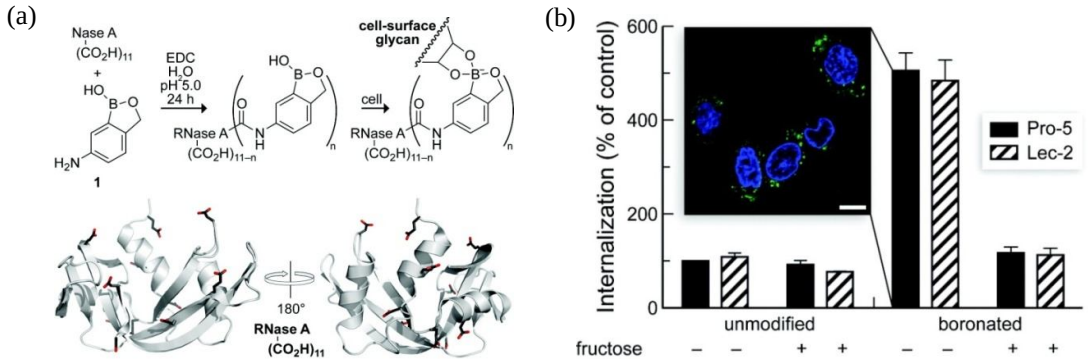

Figure 18. *(a) Boronation of RNase A and its proposed mechanism for expediting cellular delivery. The location of each carboxyl group of RNase A is depicted in the ribbon diagram. (b) Internalization of unmodified and boronated RNase A into Pro-5 and Lec-2 cells in the absence or presence of fructose. Flow cytometry data were normalized to the internalization of unmodified RNase A into Pro-5 cells. Error bars represent SDs. Inset: Confocal microscopy image of live Pro-5 cells incubated for 4 h with boronated RNase A that had been labeled covalently with a green fluorophore. Nuclei were stained blue with Hoechst 33322. Reproduced with permission from (J. Am. Chem. Soc.* ***2012****, 134, 3631). Copyright © 2012 American Chemical Society.*

Kim developed a benzoxaborole-containing styrenic monomer which can be polymerised by the reversible addition−fragmentation and chain transfer method (Scheme 3).[88] Fluorescein isothiocyanate (FITC)-labeled human insulin (F-insulin) was encapsulated within polymersomes, in order to demonstration their use as sugar-responsive containers. The strong green fluorescence of the polymersomes was observed using laser confocal fluorescence microscopy (LCFM, Figure 19). Subsequently, under physiologically relevant pH conditions, the FITC labelled insulin was released from the polymersomes in response to added monosaccharides that bind strongly with the

benzoxaborole moieties.

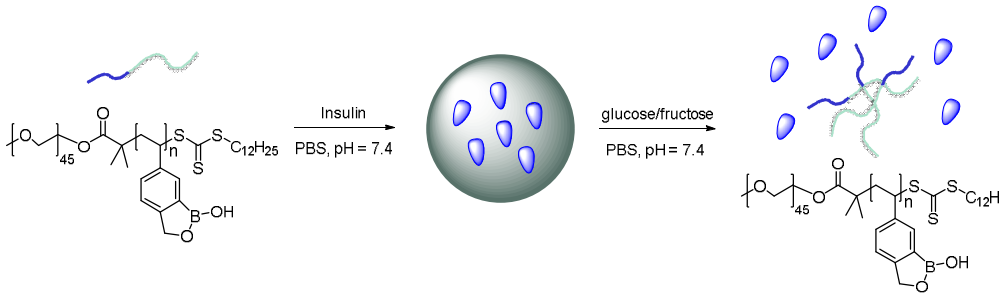

Scheme 3. *Self-assembly of PEG-b-PBOx and its disassembly in the presence of monosaccharides.*

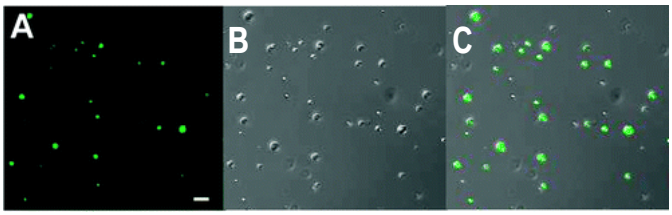

Figure 19. ***LCFM images of polymersomes of PEG-b-PBOx encapsulating FITC-labelled human insulin: (A) dark-field, (B) bright-field; (C) merged. Scale Bar: 5 µm. Reproduced with permission from (J. Am. Chem. Soc. 2012, 134, 4030). Copyright © 2012 American Chemical Society.***

Conclusions

Cellular imaging using fluorescent reporter systems for tagging cellular and subcellular processes *in vivo* have been extensively developed over the past decade but many important challenges remain, such as chemoselectivity and bioorthognity, continuous *in vivo* monitoring. It is clear that if more research can be encouraged in this area then substantial developments will be possible and these will impact the way we currently do biological research, drug discovery, and clinical practice. Especially, given the rapid development of super-resolution fluorescence microscopy (2014 Nobel Prize in chemistry), which will bolster the development of fluorescent molecular imaging for diagnostics and also the monitoring disease progression and recovery at the molecular level.[89] Carbohydrates are particularly important targets given their pivotal role in numerous important biological events, including the development and progression of many diseases. Boronic acids (BA) are a class of receptors very well suited to the binding of carbohydrates, since even the simplest BA receptors have high affinity for carbohydrates under biologically relevant conditions (in water). Putting things into perspective if boronic acid based imaging agents could aid in the development of early stage diagnostics or aid the development of treatment for just one disease such Alzheimer's disease (AD). Then, the overall economic impact would be immense, since the current economic burden of dementia per year on the UK is £26.3 billion.[90] Obviously, the answer to this problem is not going to be easy but given the rapid growth of interest in selective "fluorescence imaging" and potential of boronic acid based receptors discussed in this review we hope that solutions to these problems will be provided in the relatively near future.

Acknowledgements

XS, WZ, JSF and TDJ would like to thank The Catalysis and Sensing for our Environment (CASE) for networking opportunities.[91] XS thanks the China Scholarship Council (CSC) and University of Bath for a Full Fees Scholarship. TDJ thanks the University of Bath for support. China Scholarship Council (CSC) and the University of Birmingham are also thanked for providing studentship support (WZ). JSF thanks the

University of Birmingham for support, the Royal Society for an Industrial Fellowship and the EPSRC for funding (EP/J003220/1). JSF and TDJ are grateful for past collaborative support (DT/F00267X/1).

References

1. A. Signore, S. J. Mather, G. Piaggio, G. Malviya and R. A. Dierckx, *Chem. Rev.*, 2010, **110**, 3112-3145.
2. A. S. Stender, K. Marchuk, C. Liu, S. Sander, M. W. Meyer, E. A. Smith, B. Neupane, G. Wang, J. Li, J.-X. Cheng, B. Huang and N. Fang, *Chem. Rev.*, 2013, **113**, 2469-2527.
3. Y. Zhou, J. F. Zhang and J. Yoon, *Chem. Rev.*, 2014, **114**, 5511-5571.
4. E. L. Que, D. W. Domaille and C. J. Chang, *Chem. Rev.*, 2008, **108**, 1517-1549.
5. X.-P. He, Y. Zang, T. D. James, J. Li and G.-R. Chen, *Chem. Soc. Rev.*, 2015, **44**, 4239-4248.
6. X. Sun and T. D. James, *Chem. Rev.*, 2015, **115**, 8001-8037.
7. S. Lee, J. Xie and X. Chen, *Chem. Rev.*, 2010, **110**, 3087-3111.
8. H. Kobayashi, M. Ogawa, R. Alford, P. L. Choyke and Y. Urano, *Chem. Rev.*, 2010, **110**, 2620-2640.
9. X. Li, X. Gao, W. Shi and H. Ma, *Chem. Rev.*, 2014, **114**, 590-659.
10. M. Vendrell, D. Zhai, J. C. Er and Y.-T. Chang, *Chem. Rev.*, 2012, **112**, 4391-4420.
11. A. P. de Silva, H. Q. N. Gunaratne, T. Gunnlaugsson, A. J. M. Huxley, C. P. McCoy, J. T. Rademacher and T. E. Rice, *Chem. Rev.*, 1997, **97**, 1515-1566.
12. M. Bates, B. Huang, G. T. Dempsey and X. Zhuang, *Science*, 2007, **317**, 1749-1753.
13. R. Henriques, C. Griffiths, E. Hesper Rego and M. M. Mhlanga, *Biopolymers*, 2011, **95**, 322-331.
14. Y. Aoyama, Y. Tanaka, H. Toi and H. Ogoshi, *J. Am. Chem. Soc.*, 1988, **110**, 634-635.
15. H. E. Murrey and L. C. Hsieh-Wilson, *Chem. Rev.*, 2008, **108**, 1708-1731.
16. C. The Emerging Risk Factors, *The Lancet*, **375**, 2215-2222.
17. P. Luppi, V. Cifarelli and J. Wahren, *Pediatr. Diabetes*, 2011, **12**, 276-292.
18. N. J. Ammary-Risch, M. Aguilar, L. S. Goodman and L. Quiroz, *Fam. Community Health*, 2012, **35**, 103-110.
19. M. Rosati, M. Lisanti, A. Baluganti, L. Andreani, L. Rizzo and A. Piaggesi, *Musculoskelet. Surg.*, 2012, **96**, 191-197.
20. E. Selvin, M. W. Steffes, H. Zhu, K. Matsushita, L. Wagenknecht, J. Pankow, J. Coresh and F. L. Brancati, *N. Engl. J. Med.*, 2010, **362**, 800-811.
21. M. B. Davidson, D. L. Schriger, A. L. Peters and B. Lorber, *Jama*, 1999, **281**, 1203-1210.
22. D. McCane, R. L. Hanson, M.-A. Charles, L. T. Jacobsson, D. D. Pettitt, P. H. Bennett and W. C. Knowler, *BMJ*, 1994, **308**, 1323-1328.
23. M. Suzanne and J. R. Wands, *J. Diabetes Sci. Technol.*, 2008, **2**, 1101-1113.
24. M. P. Pereira Morais, J. D. Mackay, S. K. Bhamra, J. G. Buchanan, T. D. James, J. S. Fossey and J. M. van den Elsen, *Proteomics*, 2010, **10**, 48-58.
25. M. P. P. Morais, J. S. Fossey, T. D. James and J. M. van den Elsen, in *Protein Electrophoresis*, Springer, 2012, pp. 93-109.
26. Y. Zou, D. L. Broughton, K. L. Bicker, P. R. Thompson and J. J. Lavigne, *Chembiochem*, 2007, **8**, 2048-2051.
27. C. F. Dai, A. Sagwal, Y. F. Cheng, H. J. Peng, W. X. Chen and B. H. Wang, *Pure Appl. Chem.*, 2012, **84**, 2479-2498.

28. S. G. G. Stokes, *Rep. Br. Ass.*, 1852, 15-16.
29. M. A. Brun, K.-T. Tan, R. Griss, A. Kielkowska, L. Reymond and K. Johnsson, *J. Am. Chem. Soc.*, 2012, **134**, 7676-7678.
30. D.-S. Guo, V. D. Uzunova, X. Su, Y. Liu and W. M. Nau, *Chem. Sci.*, 2011, **2**, 1722-1734.
31. E. K. Feuster and T. E. Glass, *J. Am. Chem. Soc.*, 2003, **125**, 16174-16175.
32. J. M. West, H. Tsuruta and E. R. Kantrowitz, *J. Biol. Chem.*, 2004, **279**, 945-951.
33. K. E. Secor and T. E. Glass, *Org. Lett.*, 2004, **6**, 3727-3730.
34. J. S. Paige, T. Nguyen-Duc, W. Song and S. R. Jaffrey, *Science*, 2012, **335**, 1194-1194.
35. S. H. Shim, C. Xia, G. Zhong, H. P. Babcock, J. C. Vaughan, B. Huang, X. Wang, C. Xu, G. Q. Bi and X. Zhuang, *Proc. Natl. Acad. Sci. U S A*, 2012, **109**, 13978-13983.
36. X.-P. He, Q. Deng, L. Cai, C.-Z. Wang, Y. Zang, J. Li, G.-R. Chen and H. Tian, *ACS Appl. Mater. Interfaces*, 2014, **6**, 5379-5382.
37. E. M. Sevick-Muraca, J. P. Houston and M. Gurfinkel, *Curr. Opin. Chem. Biol.*, 2002, **6**, 642-650.
38. J. Chan, S. C. Dodani and C. J. Chang, *Nat. Chem.*, 2012, **4**, 973-984.
39. S. D. Bull, M. G. Davidson, J. M. H. Van den Elsen, J. S. Fossey, A. T. A. Jenkins, Y.-B. Jiang, Y. Kubo, F. Marken, K. Sakurai, J. Zhao and T. D. James, *Acc. Chem. Res.*, 2013, **46**, 312-326.
40. V. Ntziachristos, C. Bremer and R. Weissleder, *Eur. Radiol.*, 2003, **13**, 195-208.
41. V. Ntziachristos, J. Ripoll and R. Weissleder, *Opt. Lett.*, 2002, **27**, 333-335.
42. "smart" here means the proper design of a good sensing system with not only high sensitivity but also chemoselectivity and bioorthogonality while also the system can be easily prepared and work very well in a specific environment.
43. A. R. Lippert, G. C. Van de Bittner and C. J. Chang, *Acc. Chem. Res.*, 2011, **44**, 793-804.
44. W. Zhai, X. Sun, T. D. James and J. S. Fossey, *Chem. Asian J.*, 2015, **10**, 1836-1848.
45. X. Sun, Q. Xu, G. Kim, S. E. Flower, J. P. Lowe, J. Yoon, J. S. Fossey, X. Qian, S. D. Bull and T. D. James, *Chem. Sci.*, 2014, **5**, 3368-3373.
46. X. Sun, S.-Y. Xu, S. E. Flower, J. S. Fossey, X. Qian and T. D. James, *Chem. Commun.*, 2013, **49**, 8311-8313.
47. X. Sun, K. Lacina, E. C. Ramsamy, S. E. Flower, J. S. Fossey, X. Qian, E. V. Anslyn, S. D. Bull and T. D. James, *Chem. Sci.*, 2015, **6**, 2963-2967.
48. T. D. James, K. R. A. S. Sandanayake and S. Shinkai, *J. Chem. Soc, Chem. Commun.*, 1994, 477-478.
49. T. D. James, K. R. A. S. Sandanayake, R. Iguchi and S. Shinkai, *J. Am. Chem. Soc.*, 1995, **117**, 8982-8987.
50. T. D. James, P. Linnane and S. Shinkai, *Chem. Commun.*, 1996, 281-288.
51. A. Stephenson-Brown, A. L. Acton, J. A. Preece, J. S. Fossey and P. M. Mendes, *Chem. Sci.*, 2015, **6**, 5114-5119.
52. X. Sun, B. Zhu, D.-K. Ji, Q. Chen, X.-P. He, G.-R. Chen and T. D. James, *ACS Appl. Mater. Interfaces*, 2014, **6**, 10078-10082.
53. A. Stephenson-Brown, S. Yong, M. H. Mansor, Z. Hussein, N.-C. Yip, P. M. Mendes, J. S. Fossey and F. J. Rawson, *Chem. Commun.*, 2015, DOI: 10.1039/C5CC04311E.
54. Y. Liu, C. Deng, L. Tang, A. Qin, R. Hu, J. Z. Sun and B. Z. Tang, *J. Am. Chem. Soc.*, 2011, **133**, 660-663.

55. Y. J. Heo and S. Takeuchi, *Adv. Healthc. Mater.*, 2013, **2**, 43-56.
56. T. D. James, K. R. A. S. Sandanayake and S. Shinkai, *Angew. Chem. Int. Ed. Engl.*, 1996, **35**, 1910-1922.
57. W. Yang, S. Gao, X. Gao, V. V. R. Karnati, W. Ni, B. Wang, W. B. Hooks, J. Carson and B. Weston, *Bioorg. Med. Chem. Lett.*, 2002, **12**, 2175-2177.
58. W. Yang, H. Fan, X. Gao, S. Gao, V. V. R. Karnati, W. Ni, W. B. Hooks, J. Carson, B. Weston and B. Wang, *Chem. Biol.*, 2004, **11**, 439-448.
59. S. Craig, *Bioorg. Chem.*, 2012, **40**, 137-142.
60. C. Dai, L. H. Cazares, L. Wang, Y. Chu, S. L. Wang, D. A. Troyer, O. J. Semmes, R. R. Drake and B. Wang, *Chem. Commun.*, 2011, **47**, 10338-10340.
61. Y. Chu, D. Z. Wang, K. Wang, Z. R. Liu, B. Weston and B. H. Wang, *Bioorg. Med. Chem. Lett.*, 2013, **23**, 6307-6309.
62. X. D. Xu, H. Cheng, W. H. Chen, S. X. Cheng, R. X. Zhuo and X. Z. Zhang, *Sci. Rep.*, 2013, **3**, 2679.
63. Confocal laser scanning microscopy (CLSM) is a technique for obtaining high-resolution optical images with depth selectivity.
64. T. L. Halo, J. Appelbaum, E. M. Hobert, D. M. Balkin and A. Schepartz, *J. Am. Chem. Soc.*, 2009, **131**, 438-439.
65. K. K. Kim, J. O. Escobedo, N. N. St. Luce, O. Rusin, D. Wong and R. M. Strongin, *Org. Lett.*, 2003, **5**, 5007-5010.
66. P. M. S. D. Cal, R. F. M. Frade, V. Chudasama, C. Cordeiro, S. Caddick and P. M. P. Gois, *Chem. Commun.*, 2014, **50**, 5261-5263.
67. C.-S. Chen, X.-D. Xu, Y. Wang, J. Yang, H.-Z. Jia, H. Cheng, C.-C. Chu, R.-X. Zhuo and X.-Z. Zhang, *Small*, 2013, **9**, 920-926.
68. J. N. Cambre and B. S. Sumerlin, *Polymer*, 2011, **52**, 4631-4643.
69. W. L. A. Brooks and B. S. Sumerlin, *Chem. Rev.*, 2015, DOI: 10.1021/acs.chemrev.5b00300.
70. M. C. Roberts, M. C. Hanson, A. P. Massey, E. A. Karren and P. F. Kiser, *Adv. Mater.*, 2007, **19**, 2503-2507.
71. J. I. Jay, S. Shukair, K. Langheinrich, M. C. Hanson, G. C. Cianci, T. J. Johnson, M. R. Clark, T. J. Hope and P. F. Kiser, *Adv. Funct. Mater.*, 2009, **19**, 2969-2977.
72. C. W. Garner, *J. Biol. Chem.*, 1980, **255**, 5064-5068.
73. D. A. Matthews, R. A. Alden, J. J. Birktoft, S. T. Freer and J. Kraut, *J. Biol. Chem.*, 1975, **250**, 7120-7126.
74. G. Kahraman, O. Beşkardeş, Z. M. O. Rzaev and E. Pişkin, *Polymer*, 2004, **45**, 5813-5828.
75. L. Zhang, Y. Lin, J. Wang, W. Yao, W. Wu and X. Jiang, *Macromol. Rapid Commun.*, 2011, **32**, 534-539.
76. Y. Hu, X. Jiang, L. Zhang, J. Fan and W. Wu, *Biosens. Bioelectron.*, 2013, **48**, 94-99.
77. K. Lacina, P. Skladal and T. James, *Chem. Cent. J.*, 2014, **8**, 60.
78. Y. Zhao, B. G. Trewyn, I. I. Slowing and V. S.-Y. Lin, *J. Am. Chem. Soc.*, 2009, **131**, 8398-8400.
79. W. Wu, T. Zhou, A. Berliner, P. Banerjee and S. Zhou, *Angew. Chem. Int. Ed. Engl.*, 2010, **49**, 6554-6558.

80. Y. J. Heo, H. Shibata, T. Okitsu, T. Kawanishi and S. Takeuchi, *Proc. Natl. Acad. Sci. U.S.A.*, 2011, **108**, 13399-13403.
81. H. Shibata, Y. J. Heo, T. Okitsu, Y. Matsunaga, T. Kawanishi and S. Takeuchi, *Proc. Natl. Acad. Sci. U. S. A.*, 2010, **107**, 17894-17898.
82. M. P. Pereira Morais, D. Marshall, S. E. Flower, C. J. Caunt, T. D. James, R. J. Williams, N. R. Waterfield and J. M. van den Elsen, *Sci Rep*, 2013, **3**, 1431-1437.
83. G. Wulff, *Pure Appl. Chem.*, 1982, **54**, 2093-2102.
84. M. Dowlut and D. G. Hall, *J. Am. Chem. Soc.*, 2006, **128**, 4226-4227.
85. M. S. Shim and Y. J. Kwon, *FEBS Journal*, 2010, **277**, 4814-4827.
86. S. Patil, D. Rhodes and D. Burgess, *The AAPS Journal*, 2005, **7**, E61-E77.
87. G. A. Ellis, M. J. Palte and R. T. Raines, *J. Am. Chem. Soc.*, 2012, **134**, 3631-3634.
88. H. Kim, Y. J. Kang, S. Kang and K. T. Kim, *J. Am. Chem. Soc.*, 2012, **134**, 4030-4033.
89. K. Nienhaus and G. Ulrich Nienhaus, *Chem. Soc. Rev.*, 2014, **43**, 1088-1106.
90. http://www.alzheimers.org.uk/ (accessed November 2015)
91. J. S. Fossey and W. D. G. Brittain, *Org. Chem. Front.*, **2015**, *2*, 101-105.

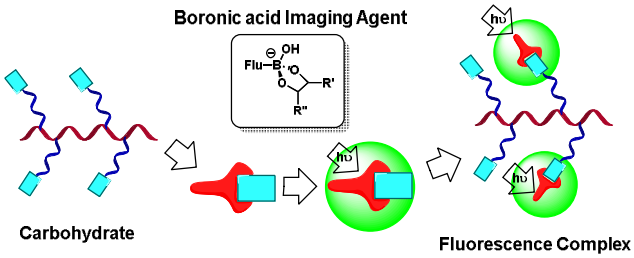

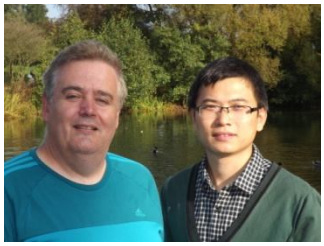

Xiaolong Sun *is now a postdoc working in Eric Anslyn's group, University of Texas at Austin, USA. He obtained his BSc from Shaanxi University of Science and Technology and MSc from East China University of Science and Technology (ECUST) under the supervision of Professor Xuhong Qian. He then became a PhD student with Tony D. James (Chemosensors Group) in the Department of Chemistry at the University of Bath. Research interests include organic synthesis for the preparation of small molecules, which can be used to understand and exploit biological systems, and in particular for the fluorescence detection of reactive species (oxygen and nitrogen) and carbohydrates.*

Tony D. James *a Professor at the University of Bath; was awarded a BSc from UEA (1986) and PhD in 1991 from the University of Victoria. He worked in Japan from 1991-1995 as a PDRF with Seiji Shinkai. From 1995 to 2000 he was a Royal Society Research Fellow at University of Birmingham. In 2000 he moved to the Department of Chemistry at the University of Bath. He has been awarded the titles of visiting professor at Tsukuba, Osaka and Kyushu Universities and guest Professor at East China University of Science and Technology (ECUST), Xiamen University, Shandong Normal University, and Nanjing University, he was also awarded a Hai-Tian (Sea-Sky) Scholarship by Dalian University of Technology. Research interests include molecular recognition, self-assembly and molecular sensor development. His research has particularly concentrated on boronic acid based receptors for the sensing and detection of carbohydrates.*

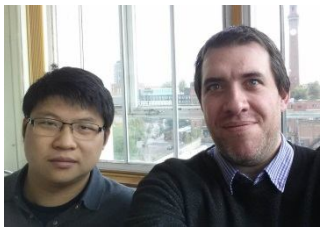

Wenlei Zhai *obtained his B. Eng. degree from China Pharmaceutical University and MSc degree from East China University of Science and Technology, working with Professor Yi-Tao Long in the area of surface-enhanced Raman spectroscopy. He joined the research group of Dr J. S. Fossey three years ago where his project involves the use of click chemistry to assemble multifunctional chemosensors.*

John S. Fossey *is a Royal Society Industry Fellow and Senior Lecturer and at the University of Birmingham, UK. He gained an MChem degree at Cardiff University of Wales in 2000, and then obtained a PhD from Queen Mary University of London in 2004, working in the group of Dr C. J. Richards. He next took up a postdoctoral position at the University of Tokyo with Professor S. Kobayashi. After three years at the University of Bath he took up his first permanent position at the University of Birmingham and was recently promoted to the position of Senior Lecturer. He enjoys collab orative projects and research themes of molecular recognition and asymmetric catalysis, applied to disease detection and treatment, agrochemicals and novel materials.*